THE JOURNAL OF PHYSICAL CHEMISTRY B LETTERS

XXXX, xxx, 000

Coaxial Cross-Diffusion through Carbon Nantoubes

Javier Rodriguez,[†,‡] M. Dolores Elola,[†] and Daniel Laria*[,†,§]

Departamento de Física, Comisión Nacional de Energía Atómica, Avenida Libertador 8250, 1429 Buenos Aires, Argentina, ECyT, UNSAM, Martín de Irigoyen 3100, 1650 San Martín, Provincia de Buenos Aires, Argentina, and Departamento de Química Inorgánica, Analítica y Química-Física e INQUIMAE, Facultad de Ciencias Exactas y Naturales, Universidad de Buenos Aires, Ciudad Universitaria, Pabellón II 1428, Buenos Aires, Argentina

Received: September 16, 2009; Revised Manuscript Received: October 5, 2009

We present results from nonequilibrium molecular dynamics experiments describing the relaxation of local concentrations at two reservoirs, initially filled with water (W) and acetonitrile (ACN), as they become connected through a membrane composed of (16,16) carbon nanotubes. Within the hydrophobic nanotube cavities, the equilibrium concentrations contrast sharply to those observed at the reservoirs, with a clear enhancement of ACN, in detriment of W. From the dynamical side, the relaxation involves three well-differentiated stages; the first one corresponds to the equilibration of individual concentrations within the nanotubes. An intermediate interval with Fickian characteristics follows, during which the overall transport can be cast in terms of coaxial opposite fluxes, with a central water domain segregated from an external ACN shell, in close contact with the tube walls. We also found evidence of a third, much slower, mechanism to reach equilibration, which involves structural modifications of tightly bound solvation shells, in close contact with the nanotube rims.

Since their discovery by Iijima in 1991,[1] the interest in carbon nanotubes (CNTs) has experienced a remarkable increase. This growth responds to their versatility as key elements in a wide variety of practical applications, which include the design of substrates for gas storage,[2] nanopipets,[3] nanotweezers,[4] agents for controlled drug delivery,[5] selective sieves,[6] and nanoelectronic devices.[7] In many of these applications, nanotubes are incorporated as building blocks of more complex structures of mesoscopic dimensions. For example, Jirange et al.[6] have recently synthesized polycarbonate membranes containing monodisperse nanotubes that allow the selective control of the flow of small solutes, based on the simple consideration of their overall molecular sizes. In a related context, Hinds and collaborators[8] have reported ionic flux control through aligned CNT membranes, operated by proper functionalization at their tip entrances as well. From a biological perspective, recent computer simulation results[9] would also indicate the possibility of intercalating pores within lipidic bilayers, via the insertion of nanotubes with hydrophilic functionalization at their rims. These results open interesting possibilities for the design of synthetic channels in membranes and, at the same time, provide appropriate benchmarks for the interpretation of much more complex phenomena, such as the transport through transmembrane ion channels.[10]

In all of these examples, the correct characterization of the diffusive motions within the tubular cavities is of primary importance. At present, there exists a large body of research work devoted to the analysis of the transport of molecular fluids through CNTs. In a broad context, the studies have focused on the analysis of diffusive modes of confined and/or adsorbed gases[11−16] and liquid-like phases[17−27] as well. Given its singular role in nature, in most of the latter studies, water has been the usual solvent choice,[28] although nonprotic solvents[25] and water−methanol mixtures have also been examined.[26]

In this Letter, we will present results from nonequilibrium molecular dynamics experiments that model the relaxation following the process of bringing together two macroscopic polar phases, comprising fully miscible protic/aprotic liquids, water (W) and acetonitrile (ACN), separated by a CNT membrane. Our research is mainly motivated by two recent simulation studies. On the one hand is the analysis performed by Karla et al.[27] pertaining to the characteristics of water flows through narrow CNT membranes, driven by osmotic gradients. On the other hand is a recent Letter by Kagulin et al.,[25] in which the diffusive behavior and the rotational dynamics of ACN confined within a single CNT of different diameters have been examined. As we will show, the characteristics of the hydrophobic confinement provided by the CNT cavities introduce distinctive characteristics in the spatial correlations and in the dynamic flows which are absent in analysis performed on the pure liquids.

The systems under investigation were composed of $N_W = 2538$ water molecules and $N_A = 586$ ACN molecules, confined within a fully periodic, rectangular box of linear dimensions $L_x = 49.3$ Å $\times$ $L_y = 41.6$ Å $\times$ $L_z = 81.5$ Å. Along the z-axis, the box is comprised of two reservoirs (I

* To whom correspondence should be addressed. E-mail: dhlaria@cnea.gov.ar.
[†] Comisión Nacional de Energía Atómica.
[‡] UNSAM.
[§] Universidad de Buenos Aires.

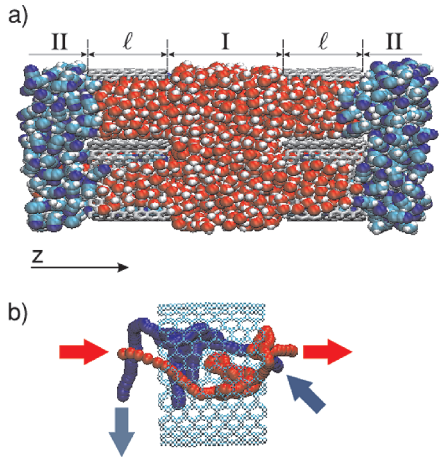

Figure 1. (a) Initial configuration for a nonequilibrium run. (b) Typical 0.5 ns diffusive trajectories for W (blue) and ACN (red) within the CNT.

and II) of similar volume V, separated by two membranes, each one containing four (16,16) armchair CNTs. The tubes are aligned with their axes parallel to the z direction; along the $x-y$ plane, the centers of the tubes are distributed in a close-packed hexagonal arrangement. Originally, reservoir I (II) was filled with W (ACN) and spanned the $|z| \leq 12.75$ Å ($|z| \geq 28.0$ Å) interval. The radii and the lengths of the CNTs were set to $R = 10.6$ Å and $l = 15.25$ Å, respectively (see Figure 1). The water Hamiltonian corresponded to the classical SPC/E model,[29] whereas parameters for the ACN were taken from the nonrigid model developed by Grabuleda et al.[30] The parametrization of the potential involving CNT sites was taken from the CHARMM library.[31]

The three panels of Figure 2 present results extracted from one typical relaxation run for $N_\alpha^i(t)$ (α = W, ACN), the population relaxations in each of the three sections (i = I, II, CNT) comprising the simulation box. In particular, the plots of the top panel correspond to results for the inner part of one typical nanotube. After a transient time of $\tau_0 \sim 5$ ns, both populations level off at equilibrium compositions well differentiated from the global one. Note that, while the overall concentration ratio of the system is $N_{ACN}/N_W = 0.23$, the relation within the nanotubes presents the opposite trend as they appear filled preferentially with ACN, $N_{ACN}^{CNT}(t = 20\ ns)/N_W^{CNT}(t = 20\ ns) \sim 1.7$. The enhancement in the local concentration of ACN is the result of the combined effects arising from the restricted geometry and the characteristics of the CNT−solvent interactions, which are dominated by dispersion forces. As such, the present situation resembles very much the one observed by us in a recent simulation study of similar mixtures confined within two hydrophobic silica plates, held fixed at typical distances on the order of 1 nm.[32]

Given these characteristics, it is of interest to analyze the density fields within the CNT cavities. In the top panel of Figure 3, we present a snapshot of a typical configuration of the solvent distributions in these regions. At a first glance, it is self-evident that the overall structure can be cast in terms of a central water domain segregated from an external layer of ACN, in close contact with the CNT wall. We remark that such a structure was found at practically all times, following the initial equilibration period, even though the concentrations at the external reservoirs were far from being equilibrated. In the snapshot, one also observes ACN molecules getting through the interstices equidistant from three neighboring tubes, which are narrow enough to accommodate only a single, perfectly aligned, "chain"

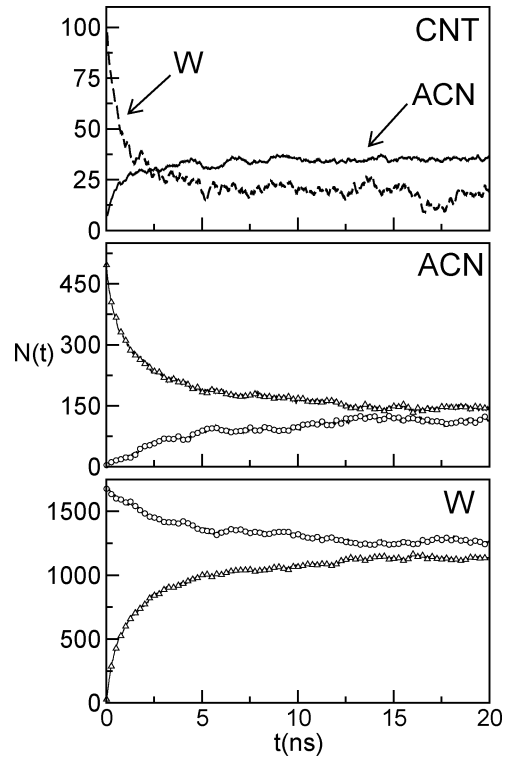

Figure 2. Concentration relaxations in different environments. Top panel: CNT. Middle panel: ACN relaxations. Bottom panel: W relaxations. (Reservoir I: circles; reservoir II: triangles.)

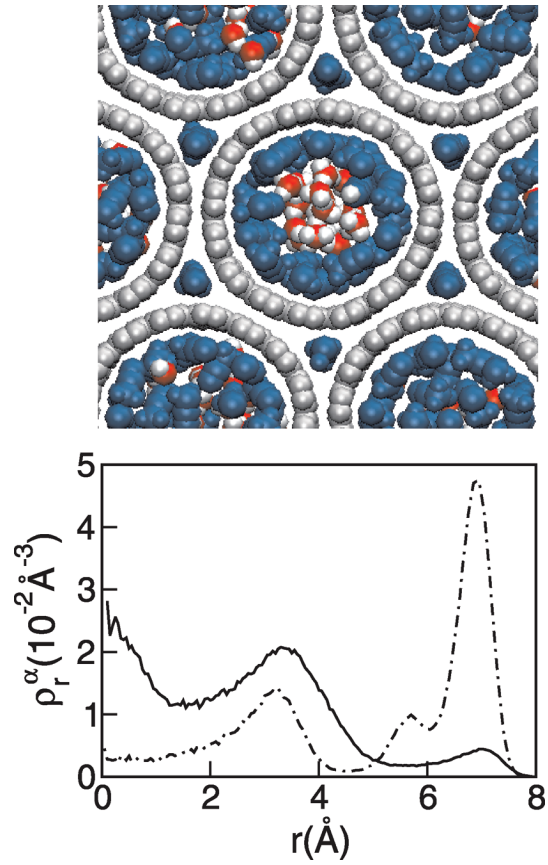

Figure 3. Top panel: Snapshot of a section of filled CNT. Bottom panel: Density fields of each species across the sections of the CNT. (W: solid line; ACN: dot−dashed line.)

of ACN.[33] No water was observed to permeate through these much narrower cavities.

In the bottom panel of Figure 3, the latter structural features are analyzed on more quantitative grounds. The plots correspond to density fields $\rho_r^\alpha(r)$ computed as

$$\rho_r^\alpha(r) = \frac{1}{l\pi r^2}\left\langle \sum_i \delta(r_i^\alpha - r)\right\rangle \quad (1)$$

where the sum is restricted to those molecules lying at the interior of a tagged CNT and r_i^α represents the distance from the ith particle of species α to the axis of the cylindrical nanotube (α is the central C atom for ACN and the O atom for W). Clearly, the confinement prevailing in the nanotube cavity imposes a considerable degree of structure in the distributions of both fluids; the W profile presents two main peaks, one at $r \sim 0$ Å and a second one at $r = 3.8$ Å, whereas the ACN localizes mainly at $r \sim 7$ Å and, to a much lesser extent, at $r \sim 3$ Å. In passing, we note that these tubes exhibit perhaps the smallest radii that allow for hosting the two solvents. Similar experiments performed with CNTs of smaller diameters show cavities completely deprived of W and filled exclusively with ACN,[34] a feature that is akin to the drying episodes that have been observed at the interior of small nanotubes immersed in water.[35]

In the central and bottom panels of Figure 2, we present results for the concentration relaxations of the solvents within the two reservoirs. The modifications during the first 5 ns are dominated by the drain of ACN out of reservoir II and the concomitant incorporation of W. Both phenomena involve diffusive motions along the nanocavities, in opposite directions. For $t \gtrsim \tau_0$, as expected, the fluxes in and out of each reservoir practically compensate for each other. The joint consideration of the structural and the dynamical characteristics of the transport leads now to a scenario in which the overall relaxation is operated by coaxial fluxes, exhibiting opposite directions. Figure 1b shows two typical trajectories for representative W and ACN molecules that clearly describe this feature.

We further analyzed the characteristics of the diffusive motions, exploring whether a temporal regime exists during which the fluxes might exhibit Fickian characteristics. Within the realm of linear theories for multicomponent systems, the macroscopic diffusive flux of species α, J_α, is defined in terms of the diffusivities, $D_{\alpha\gamma}$, and concentration gradients, namely[36]

$$J_\alpha = -\sum_\gamma D_{\alpha\gamma}\nabla c_\gamma \quad (2)$$

At the lowest level of approximation

$$\nabla c_\alpha \sim \frac{\Delta\bar{N}_\alpha(t)}{Vl} = \frac{\bar{N}_\alpha^k(t) - \bar{N}_\alpha^j(t)}{Vl} \qquad J_\alpha \sim \frac{1}{A_\alpha}\left[\frac{\partial\bar{N}_\alpha^k(t)}{\partial t}\right] \quad (3)$$

Moreover, considering the extent of segregation observed between the two species within the nanotubes, it is reasonable to speculate that the fluxes of W and ACN should be weakly coupled. If so, from eqs 2 and 3, the expression for the population relaxations in each reservoir would be

$$\Delta\bar{N}_\alpha(t) \sim -\frac{lV}{D_\alpha}\frac{1}{A_\alpha}\left[\frac{\partial\bar{N}_\alpha^k(t)}{\partial t}\right] = -K_\alpha\left[\frac{\partial\bar{N}_\alpha^k(t)}{\partial t}\right] \quad (4)$$

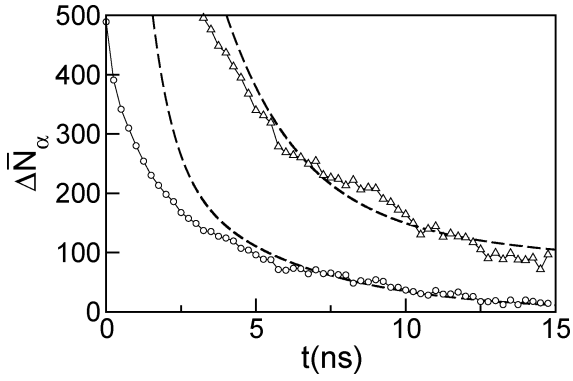

Figure 4. Nonequilibrium relaxations of the gradient of concentration for ACN (circles) and W (triangles). The dashed lines correspond to predictions from linear models.

In the previous equations, D_α and A_α stand for the "effective" diffusion coefficient throughout the tubes and the "effective" section of CNT available for transport of species α, respectively. The bars indicate an average taken from an ensemble of nonequilibrium initial conditions.[37]

Results for $\Delta\bar{N}_\alpha(t)$ for W and ACN are depicted in Figure 4, along with predictions from Fick law obtained by adjusting the prefactors in the last term of eq 4 to $K_W = 14.8$ ns and to $K_{ACN} = 9.4$ ns, so as to yield reasonable matches between the long time portions of the two sets of curves. Note that in doing so, Fick law's predictions seem to remain valid starting at $t \sim 5$ ns and beyond. Given the approximations involved in deriving eq 4, the quality of the agreement is rather unexpected. Moreover, note that at $t \sim 5$ ns, the generalized forces that drive the individual diffusions, expressed in terms of $\Delta\bar{N}_W(t\sim5\text{ ns})/\bar{N}_W(t\to\infty) \sim 0.2$ and $\Delta\bar{N}_{ACN}(t\sim5\text{ ns})/\bar{N}_{ACN}(t\to\infty) \sim 0.8$ are not that small compared to unity either. Consequently, our results would suggest that the onset for the validity of linear theories would be dictated to a large extent by the equilibration of the concentrations in the CNT channels and that their predictions remain robust even for relatively large concentration gradients.

It is also possible to predict the order of magnitude of the prefactors K_α via an independent route that involves the direct consideration of a few relevant geometrical parameters of the system and the diffusion coefficients of the two components within the nanotube. From the plots of Figure 3, it is reasonable to assume that the effective areas for confined W and ACN are of similar magnitude, both being on the order of 8 × half of the total section of each nanotube, say, $A_W \sim A_{ACN} \sim 1.3 \times 10^3$ Å^2. As the individual diffusion coefficients are concerned, should the behaviors of the confined pure liquids remain comparable to those observed here, they should also be on the order of ∼50−100 Å^2 ns^{-1}.[38] As such, armed with these estimates, one obtains $K_\alpha \sim 8.2$ ns, a value quite close to the two values of K_α reported above. Given the crude nature of our simple calculations, this observation would bring additional support to the validity of linear models.

The curves of Figure 2 reveal that, even after ∼20 ns, concentrations at the two reservoirs are not totally equilibrated. This observation suggests the persistence of a third, much slower, mechanism that would drive the final stages of the relaxations. Looking for possible clues that would help us to identify the nature of such processes, we investigated the solvent densities at both reservoirs along two 1 ns time intervals at $t = 10$ and at 20 ns. In Figure 5, we present the results in terms of density fields of the type

$$\rho_\alpha(z) = \frac{1}{L_xL_y}\sum_i \langle\delta(z_\alpha^i - z)\rangle \quad (5)$$

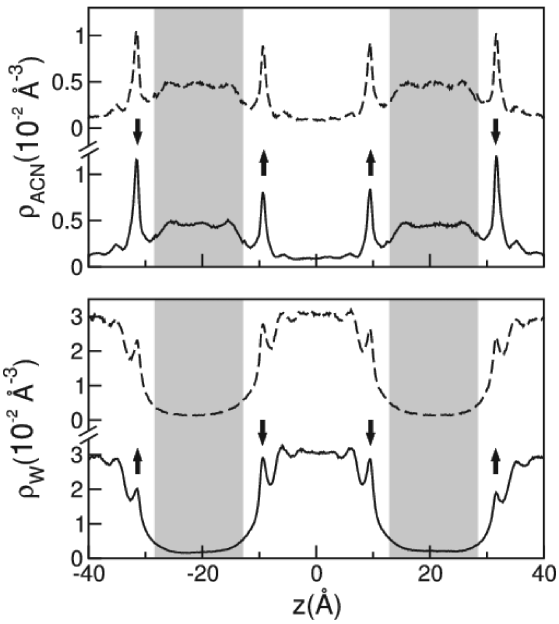

Figure 5. Nonequilibrium density fields along the z-axis of the simulation box for ACN (top panel) and W (bottom panel) at two different times, $t \sim 10$ (solid lines) and 20 ns (dashed lines). The shaded areas correspond to the location of the membranes, and the arrows indicate the trends of the changes operated at the tightly bound solvent layers at the CNT rims.

In all cases, the profiles are dominated by four peaks located at $z \sim \pm 9.8$ and ± 31 Å that correspond to solvent tightly bound to the CNT rims. Note, however, that at $t = 10$ ns, while the densities at the "bulk" portions of the reservoirs seem to be equilibrated, the magnitude of the main peaks in the two reservoirs are still different (this feature is more vivid in ACN than in W). Results for $t = 20$ ns (dashed lines) show that the only relevant changes that have operated during the last 10 ns of the trajectory are those affecting the lateral peaks, which now look somewhat more comparable than those at $t = 10$ ns. Given these circumstances, the final stages of the equilibrations would involve W and ACN detachments from the rims, followed by the diffusion through the tubes. Moreover, the magnitude of the time scales characterizing these processes suggests that they should involve the passage over a non-negligible free energy barrier, compared to normal thermal energies. Estimations of these much longer time scales normally require the implementation of a biased sampling procedure, an analysis which is well beyond the scope of the present work.

Summarizing, the results presented in this Letter shed light on several interesting features pertaining to the behavior of W−ACN mixtures confined within CNTs. In particular, in the tubular cavities, we found strong local concentration fluctuations promoted by the combined effects of the restricted geometry and the prevalence of hydrophobic interactions. On the other hand, from the dynamical side, the main conclusion concerns the robustness of linear response predictions, despite the complexities of the above-mentioned local density fluctuations within the nanotube cavities. There are several relevant questions which remain unanswered concerning the physical picture presented here. Most notably are those concerning possible effects derived from the presence of polar groups at the tube rims. Given the distinctive solvation characteristics of cations and anions in bulk protic−aprotic mixtures[39] and the flux control exerted by different polar species lying at the CNT gates that have been observed in previous experiments[40] and simulation studies,[26] one can anticipate a rich variety of solvation scenarios within CNT cavities worth investigating.

Acknowledgment. We are indebted to R. Fernández-Prini for many fruitful discussions concerning the contents of this paper.

Supporting Information Available: Additional technical details concerning the simulation procedure. This material is available free of charge via the Internet at http://pubs.acs.org.

References and Notes

(1) Iijima, S. *Nature* **1991**, *363*, 603.
(2) Liu, C.; Fan, Y. Y.; Liu, M.; Cong, H. T.; Cheng, H. M.; Dresselhaus, M. S. *Science* **1999**, *286*, 1127.
(3) Hwang, H. J.; Byum, K. R.; Kang, J. W. *Physica E* **2004**, *23*, 208.
(4) Kim, P.; Lieber, C. M. *Science* **1999**, *286*, 2148.
(5) Singh, R.; Pantarotto, D.; Lacerda, L.; Pastorin, G.; Klumpp, C.; Prato, M.; Bianco, A.; Kostarelos, K. *Proc. Natl. Acad. Sci. U.S.A.* **2006**, *103*, 3357.
(6) Jirage, K. B.; Hulteen, J. C.; Martin, C. R. *Science* **1997**, *278*, 655.
(7) Sazonova, V.; Yaish, Y.; Ustunel, H.; Roundy, D.; Arias, T. A.; McEuen, P. L. *Nature* **2004**, *287*, 622.
(8) Hinds, B. J.; Chopra, N.; Rantell, T.; Andrews, R.; Gavalas, V.; Bachas, L. G. *Science* **2004**, *303*, 62. Majunder, M.; Zhan, X.; Adnrews, R.; Hinds, B. J. *Langmuir* **2007**, *23*, 8624.
(9) Lopez, C. F.; Nielsen, S. O.; Moore, P. B.; Klein, M. L. *Proc. Natl. Acad. Sci. U.S.A.* **2004**, *101*, 4431.
(10) See, for example: Aquaporins. In *Current Topics in Membranes*; Hohmann, S., Agre, P., Nielse, S., Benos, D. J., Simon, S. A., Eds.; Academic Press: San Diego, CA, 2001; Vol. 51.
(11) (a) Kamala, C. R.; Ayappa, K. G.; Yashonath, S. *J. Phys. Chem. B* **2004**, *108*, 4411. (b) Kamala, C. R.; Ayappa, K. G.; Yashonath, S. *Phys. Rev. E* **2002**, *65*, 061202.
(12) (a) Mao, Z.; Sinnott, S. B. *J. Phys. Chem. B* **2001**, *105*, 6916. (b) Lee, K.-H.; Sinnott, S. B. *Nano Lett.* **2005**, *5*, 793. (c) Mao, Z.; Sinnott, S. *Phys. Rev. Lett.* **2002**, *27*, 278301.
(13) Hung, L.; Zhang, L.; Shao, Q.; Lu, L.; Lu, X.; Jiang, S.; Shen, W. *J. Phys. Chem. C* **2007**, *111*, 11912.
(14) Muris, M.; Dufau, N.; Bienfait, M.; Dupont-Pavlovsky, N.; Grillet, Y.; Palmari, J. P. *Langmuir* **2000**, *16*, 7019.
(15) (a) Chen, H.; Scholl, D. S. *J. Am. Chem. Soc.* **2004**, *126*, 7778. (b) Skoulidas, A. I.; Bowen, T. C.; Doelling, C. M.; Falconer, J. L.; Noble, R. D.; Scholl, D. S. *J. Membr. Sci.* **2003**, *227*, 123. (c) Skoulidas, A. I.; Ackermann, D. M.; Johnson, J. K.; Sholl, D. S. *Phys. Rev. Lett.* **2002**, *89*, 185901.
(16) Krishna, R.; van Baten, J. M. *Ind. Eng. Chem. Res.* **2006**, *45*, 2084.
(17) Holt, J. K.; Park, H. G.; Wang, Y.; Stadermann, M.; Artyukin, A. B.; Grigoropoulos, C. P.; Noy, A.; Bakajin, O. *Science* **2006**, *312*, 1034.
(18) Striolo, A. *Nano Lett.* **2006**, *6*, 633.
(19) Huang, L.-L.; Zhang, L.-Z.; Shao, Q.; Wang, J.; Lu, L.-H.; Lu, X.-H.; Jian, S.-Y.; Shen, W.-F. *J. Phys. Chem. B* **2006**, *110*, 25761.
(20) Thomas, J. A.; McGaughey, A. J. H. *Phys. Rev. Lett.* **2009**, *102*, 184502.
(21) Lui, Y.; Wang, Q. *Phys. Rev. B* **2005**, *72*, 085420.
(22) (a) Martí, J.; Gordillo, C. *J. Chem. Phys.* **2001**, *114*, 10488. (b) Martí, J.; Gordillo, C. *J. Chem. Phys.* **2003**, *119*, 12540.
(23) Maibaum, L.; Chandler, D. *J. Phys. Chem. B* **2003**, *107*, 1189.
(24) Chen, X.; Cao, G.; Han, A.; Punyamurtula, V. K.; Liu, L.; Culligan, P.; Kim, T.; Qiao, Y. *Nano Lett.* **2008**, *8*, 2988.
(25) Kagulin, O. N.; Chaban, V. V.; Loskutov, V. V.; Prezhdo, O. V. *Nano Lett.* **2008**, *8*, 2126.
(26) Zhen, J.; Lennon, E. M.; Taso, H.-K.; Sheng, Y.-J.; Jiang, S. *J. Chem. Phys.* **2005**, *122*, 214702.
(27) Karla, A.; Garde, S.; Hummer, G. *Proc. Natl. Acad. Sci. U.S.A.* **2003**, *100*, 1017.
(28) For a recent review article on water in CNTs, see, for example: Alexiadis, A.; Kassinos, S. *Chem. Rev.* **2008**, *108*, 5104.
(29) Berendsen, H. J. C.; Grigera, J. R.; Straatsma, T. P. *J. Phys. Chem.* **1987**, *91*, 6269.
(30) Grabuleda, X.; Jaime, C.; Kollman, P. A. *J. Comput. Chem.* **2000**, *21*, 901.
(31) MacKerell, A. D., Jr.; Bashford, D.; Bellott, M.; Dunbrack, R. L., Jr.; Evanseck, J. D.; Field, M. J.; Fischer, S.; Gao, J.; Guo, H.; Ha, S.; Joseph-McCarthy, D.; Kuchnir, L.; Kuczera, K.; Lau, F. T. K.; Mattos, C.; Michnick, S.; Ngo, T.; Nguyen, D. T.; Prodhom, B.; W. E.; Reiher, W. E., III.; Roux, B.; Schlenkrich, M.; Smith, J. C.; Stote, R.; Straub, J.; Watanabe, M.; Wiórkiewicz-Kuczera, J.; Yin, D.; Karplus, M. *J. Phys. Chem. B* **1998**, *102*, 3586.

(32) Rodriguez, J.; Elola, M. D.; Laria, D. *J. Chem. Phys. B* **2009**, *113*, 12744.

(33) Intersticial ACN molecules clearly exhibit a single-file diffusive mechanism which contrasts with the one observed for the rest of the molecules filling the nanotubes. Yet, their overall dynamics is sufficiently slow so as to be able to discard any relevant modifications in our dynamical analysis arising from this additional relaxation channel.

(34) Rodriguez, J.; Elola, M. D.; Laria, D. To be published.

(35) (a) Hummer, G.; Rasaiah, J. C.; Noworyta, J. P. *Nature* **2001**, *414*, 188. (b) Waghe, A.; Rasaiah, J.; Hummer, G. *J. Chem. Phys.* **2002**, *117*, 10789.

(36) Taylor, R.; Krishna, R. *Multicomponent Mass Trasfer*; Wiley & Sons: New York, 1993.

(37) See Chandler, D. *Introduction to Modern Statistical Mechanics*; Oxford University Press: New York, 1987, Chapter 8.

(38) (a) The individual diffusion coefficients of equimolar, bulk ACN−W solutions are comparable, both on the order of $\sim$300 Å^2 ns^{-1}. See: von Goldammer, E.; Hertz, H. G. *J. Phys. Chem.* **1970**, *74*, 3734. (b) Under confinement, these coefficients drop down by a factor of $\sim$3−4; see ref 25 and Liu, Y.; Yuang, Q. *Phys. Rev. B* **2005**, *72*, 085420.

(39) See, for example: Hefter, G. *Pure Appl. Chem.* **2005**, *77*, 605.

(40) Fornasiero, F.; Park, H. G.; Holt, J. K.; Stadermann, M.; Grigoropoulos, C. P. *Proc. Natl. Acad. Sci. U.S.A.* **2008**, *105*, 17250.

JP908971B